CHARACTERIZATION OF 3D FIBRE DISTRIBUTION WITHIN DISCONTINUOUS-FIBRE REINFORCED POLYMER MATRIX COMPOSITES USING FIBRE CELLS

Zhou, Y[12], Hubert, P[12]*
[1] Mechanical Engineering, McGill University, Montreal, Canada
[2] Research Centre for High Performance Polymer and Composite Systems, Montreal, Canada
* Pascal Hubert (pascal.hubert@mcgill.ca)

Keywords*: Short fibre composites; Microstructures; Machine learning*

ABSTRACT

Discontinuous-fibre reinforced polymer matrix composites (DFR PMCs) are increasingly used in the automotive industry to achieve lightweight design of vehicles. The fibre distribution within the DFR PMCs has a strong influence on their mechanical properties and therefore the characterization of the fibre distribution is key to the mechanical property predictions of the DFR PMCs. Currently, the fibre distribution within DFR PMCs is commonly characterized separately by the fibre orientation distribution and the fibre length distribution, while the fibre packing states are rarely addressed. The objective of this study is to develop a characterization framework that can spontaneously address the fibre packing states, the fibre orientation distribution, and the fibre length distribution within the DFR PMCs. The new framework is based on the concept of fibre cell. The distribution aspects of each fibre are described by the properties of its fibre cell so that the fibre distribution within the whole fibre domain can be characterized solely based on the fibre cell properties. In addition, the correlation between the fibre distribution characterized by the new framework and their corresponding material properties are established using an artificial neural network.

1 INTRODUCTION

In recent years, discontinuous-fibre reinforced polymer matrix composites (DFR PMCs) are increasingly adopted in the automotive industry to achieve lightweight vehicle designs. The fibre distribution within the DFR PMCs has a strong influence on their mechanical properties [1,2]. The multiscale finite element analysis is commonly used to predict the mechanical properties of DFR PMCs. Specifically, representative volume elements (RVEs) are used to compute the homogenized material properties based on the microscale fibre distribution at a local level. Then, macroscale analysis can be performed at the component level based on the homogenized material properties at the local level provided by the RVEs. Nevertheless, as RVEs are usually finite element based, their computational cost is very high and constructing a RVE for each different microscale fibre layout is therefore unrealistic. To reduce the computational cost of the RVEs, surrogate models are usually created based on a RVE database. The surrogate models predict the homogenized material properties of a given RVE based on the similarities between the fibre distribution within the given RVE and the fibre distribution within the RVEs in the database. An accurate characterization of the fibre distribution is therefore key to the performance of the surrogate models. From the literature, the fibre distribution within DFR PMCs is characterized by three major aspects, namely, the fibre volume fractions, the fibre orientations and the fibre lengths [3,4]. There is no established method to characterize the fibre packing states within the DFR PMCs. Besides, all fibre distribution aspects are characterized separately, while the links between each aspect are rarely studied. In this paper, a new method is proposed to characterize the fibre distribution within DFR PMCs. Compared with traditional characterization methods, the proposed method can address the fibre packing states in addition to the three major fibre distribution aspects. Besides, all fibre distribution

aspects are characterized in a joint manner unlike the traditional methods which characterize each fibre distribution aspect separately. Furthermore, the proposed characterization method is integrated with an artificial neural network (ANN) to acquire the correlation between the fibre distribution and the homogenized elastic modulus, so that the ANN can later be used as a surrogate model to provide fast homogenized elastic modulus predictions based on the fibre distribution information.

2 SAMPLE GENERATION

In this study, the framework developed by Omairey et al. is used to compute the homogenized elastic modulus of RVEs with different fibre distribution [5]. The surface mesh interpolation method proposed by Nguyen et al. is also implemented to impose the periodic boundary conditions on the RVEs [6]. Both the fibres and the matrix are modelled as isotropic material. The elastic modulus and the Poisson's ratio are 350 GPa and 0.27 for the fibres and 2.1 GPa and 0.39 for the matrix. The RVE database was formed by generating 4400 RVEs. Among them, 3400 RVEs contained randomly distributed unidirectional (UD) fibres along the X-axis with a constant aspect ratio of 7.5, which means the only aspects that can differentiate these RVEs are their fibre volume fractions and their fibre packing states. The remaining 1000 RVEs contained randomly distributed non-unidirectional (non-UD) fibres with varying fibre lengths, which represent more realistic fibre distribution scenarios. The homogenized elastic modulus along the X-axis, E_{11}, as illustrated in Figure 1, was computed for each RVE to label its homogenized elastic modulus. During this study, the RVE database was divided into a training set, a validation set, and a test set. The training set and the validation set was used for the model development, and the test set was used to evaluate the model performance.

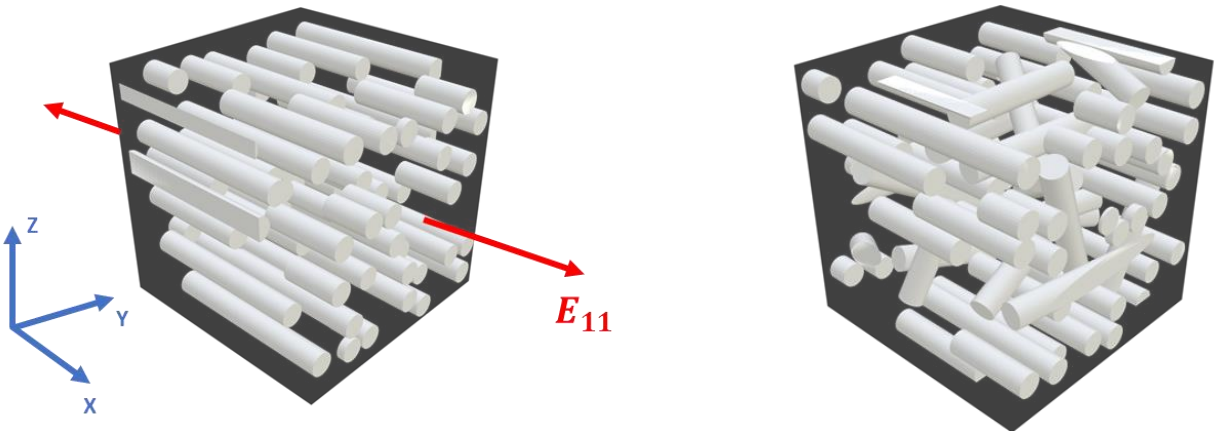

Figure 1. RVE with unidirectional fibres of identical length (left) and non-unidirectional fibres of varying lengths (right).

3 FIBRE DISTRIBUTION CHARACTERIZATION

3.1 Fibre Cell Construction

For each fibre, a fibre cell was constructed using Voronoi diagram [7]. As shown in Figure 2 with fibre cells marked in different colours, the boundary of each fibre cell is in the middle between its enclosed fibre and the neighbouring fibres. With fibre cells constructed, the packing state of each fibre is described by the size of its cell, the shape of its cell, and its relative location within its cell.

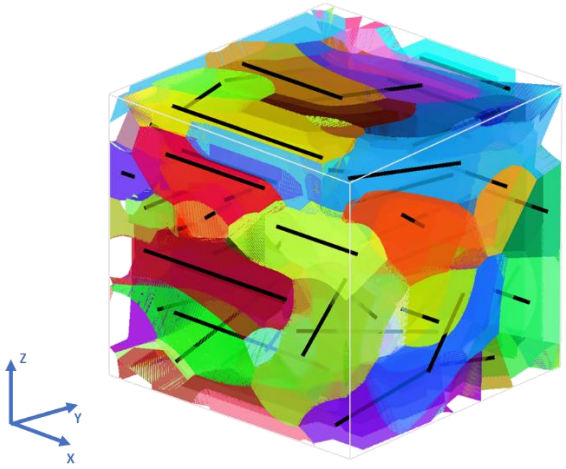

Figure 2. Visualization of fibre cells.

3.2 Fibre Cell Parameterization

To describe the fibre cells in a quantitative manner, the fibre cell properties are parameterized into 10 dimensionless parameters: the size of the fibre cell is defined by one parameter, the relative location of the enclosed fibre is defined by three parameters, and the shape of the fibre cell is defined by six parameters. Specifically, as demonstrated in Figure 3, the size of the fibre cell is defined by the local fibre volume fraction, $x_{local\ VF}$, using Equation 1. A fibre cell tends to have a high local volume fraction when its enclosing fibre has a large size or is closely surrounded by the neighbouring fibres. The relative location of the enclosed fibre in the fibre cell is described by three parameters: the fibre centroid shift, $x_{centroid\ shift}$, the fibre centroid shift angle theta, θ, and the fibre centroid shift angle phi, φ. The fibre centroid shift is defined using Equation 2, a fibre cell tends to have a larger centroid shift when the included fibre is closer to its neighbouring fibres in a certain direction, and the direction is defined by the fibre centroid shift angle theta and phi. The shape of the fibre cell was parameterized using a convolutional neural network (CNN) encoder trained via contrastive learning [8]. Specifically, the fibre cell was transformed into a 3D image first and then parameterized into six shape parameters, $x_{shape\ 1}$~$x_{shape\ 6}$, using the CNN encoder. The shape parameters will have the same values if two fibre cells have an identical shape, and the differences between the shape parameters increase with the disparities between the shapes of the fibre cells. In this way, the shapes of the fibre cells can be compared quantitatively.

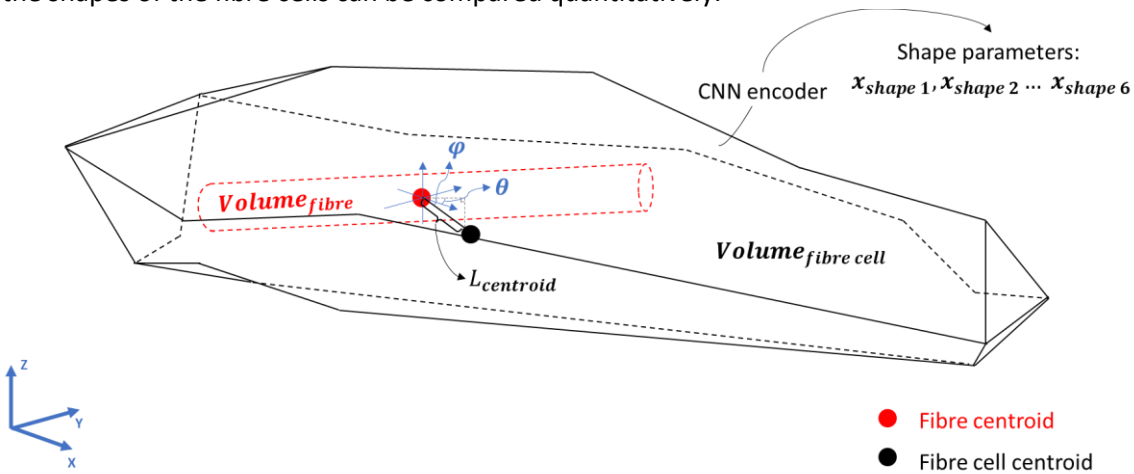

Figure 3. Fibre cell parameterization.

$$x_{local\ VF} = \frac{Volume_{fibre}}{Volume_{fibre\ cell}} \quad (1)$$

$$x_{centroid\ shift} = \frac{{L_{centroid}}^3}{Volume_{fibre\ cell}} \quad (2)$$

3.3 Fibre Cell Clustering

In an equivalent manner to the fibre orientation and length characterization, the fibre cells within a RVE can be characterized by clustering the fibre cells of similar properties into a single group. The fibre orientation and length characterization are both based on one-dimensional data; therefore, the clustering can be done linearly. However, it is not feasible to cluster fibre cells linearly because fibre cells are described by 10 parameters and therefore have a much higher dimensionality. The k-means clustering algorithm [9], which clusters data points of high dimensionalities based on their Euclidean distances in the high-dimensional space, was implemented to divide fibre cells into different clusters based on their properties. As different fibre cell parameters could have different degrees of impact on the homogenized elastic properties, all fibre cell parameters were normalized into the same scale and then assigned with weight factors to control the clustering outcomes. The number of clusters can be defined based on the needs of the users, the fibre cells can be categorized more finely by increasing the number of clusters, while the computational cost of the clustering will also rise. Considering the RVEs in the database include up to 69 fibres, the number of clusters is defined to be 60 in this study to sufficiently differentiate the fibre cells in each RVE.

4 MODEL IMPLEMENTATION

With the fibre distribution inside the RVEs characterized by the distribution of fibre cells, the correlation between the fibre cell distribution and the homogenized elastic modulus of the RVEs can be acquired using an ANN [10]. The schematic of the machine learning (ML) framework, which includes the k-mean clustering algorithm and the ANN, is shown in Figure 4. Firstly, fibre cells are constructed for the RVEs in the training and the validation set, and a CNN encoder is trained using these fibre cells. Then, the fibre cells in the RVEs from the training and the validation set are parameterized using the CNN encoder. Weight factors were applied to the fibre cell parameters, and the k-means clustering was applied to divide the fibre cells into 60 clusters based on their weighted parameters. With the clusters assigned for the fibre cells, the distribution of the fibre cells in each RVE can be represented as a histogram, each bin in the histogram represents the appearance frequency (density) of a certain fibre cell type in the RVE. Then, the correlation between fibre cell distribution and the homogenized elastic modulus of the RVE was obtained by training an ANN. Lastly, the differential evolution was applied to find the optimum weight factors for the fibre cell clustering that can minimize the error of the ANN [11].

After the optimum weight factors are obtained, the fibre distribution within any RVE can be characterized by its fibre cell distribution and the ANN can provide an instant prediction of its homogenized elastic modulus based on its fibre cell distribution.

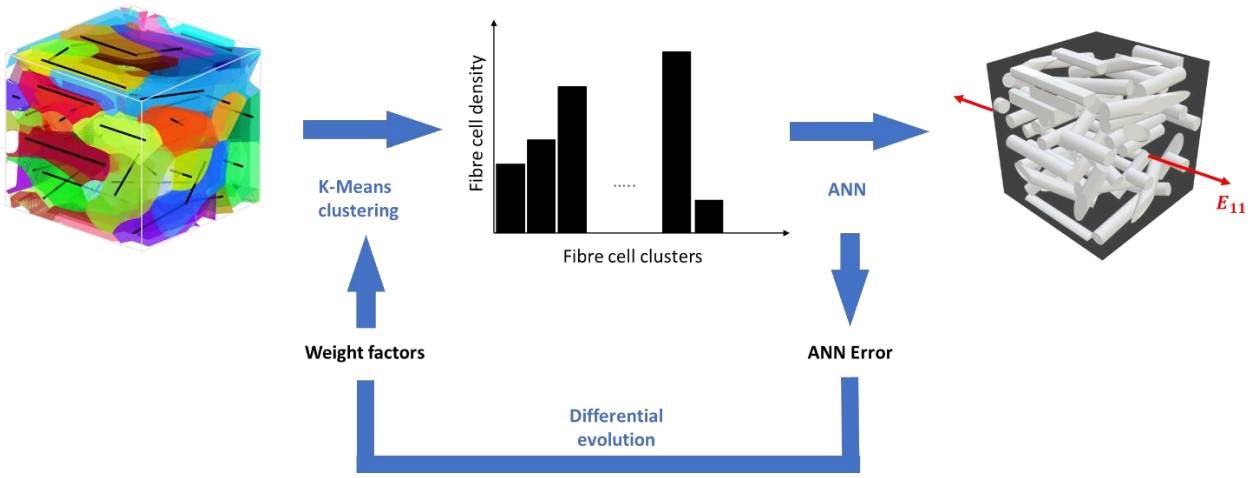

Figure 4. Framework of the ML model for instant homogenized elastic modulus predictions.

5 RESULTS

Two case studies were performed using the RVEs from the database. In the first case, 3400 UD RVEs were divided into a training set of 2800 RVEs, a validation set of 300 RVEs, and a test set of 300 RVEs. As the UD RVEs are only differentiated by their fibre volume fractions and fibre packing states, the objective of the first case was to study the influence of fibre packing states on the homogenized elastic modulus. In the second case, 1000 non-UD RVEs were mixed with 500 UD RVEs. Then, the mixed RVEs are divided into a training set of 900 RVEs, a validation set of 300 RVEs, and a test set of 300 RVEs. The objective of the second case was to test the performance of the proposed framework in a more realistic fibre distribution situation.

5.1 Unidirectional Fibres of Equal Length

The fibre volume fractions of all the UD RVEs and their corresponding finite element analysis (FEA) computed E_{11} are plotted in Figure 5. If the fibre distribution within the RVEs can be fully characterized by the fibre volume fractions, the fibre orientations, and the fibre lengths, the fibre volume fractions of the UD RVEs and their FEA computed E_{11} should have a trivial correlation. In other words, the plot in Figure 5 should be a perfect line. However, significant fluctuations in the FEA computed E_{11} can be observed from the plot. As all fibres in the UD RVEs have the same length and orientation, the variations in the FEA computed E_{11} can only be caused by the difference in the fibre packing states. In addition, the fluctuations in the FEA computed E_{11} are observed to be increasing with the fibre volume fraction as more fibres are involved in the RVEs at high volume fractions. With more fibres involved, there are consequently more potential variations in the fibre packing states and thus more significant variations in the E_{11}. Considering the number of fibres within DFR PMCs is innumerable, it seems logical to also include fibre packing states during the fibre distribution characterization.

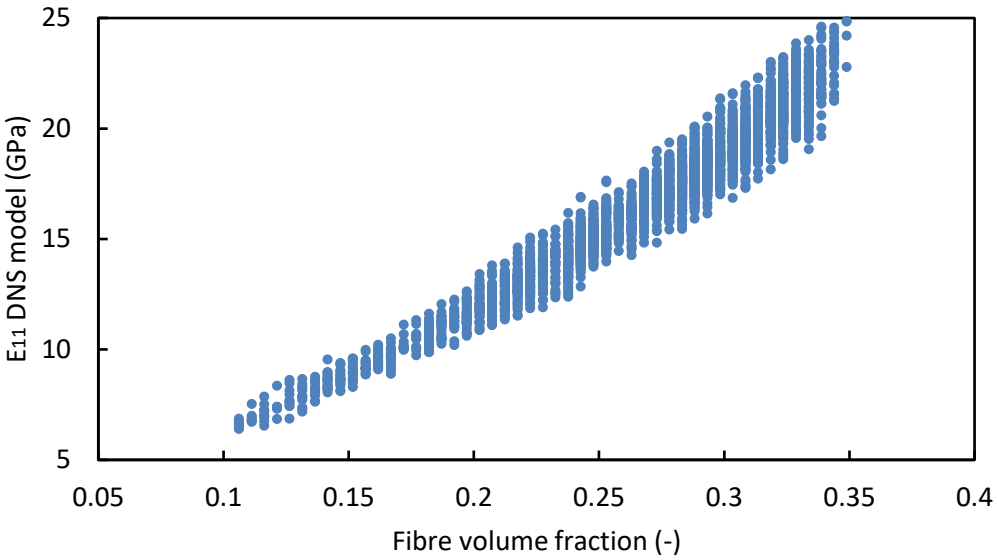

Figure 5. Correlation between fibre volume fraction and FEA computed E_{11} for UD RVE samples.

To take the fibre packing states into the consideration, the ML model based on the concept of fibre cell was used to predict the FEA computed E_{11} in the test set. For comparison purposes, a linear regression model that only includes the fibre volume fractions was constructed based on the RVEs in the training and the validation set and also used to predict the FEA computed E_{11} in the test set. The FEA computed E_{11} versus surrogate model predicted E_{11} plots are shown in Figure 6 for both cases. A red line with the slope of 1 and intercept of 0 is also plotted on each figure, all points should be on this line if the surrogate model was perfect.

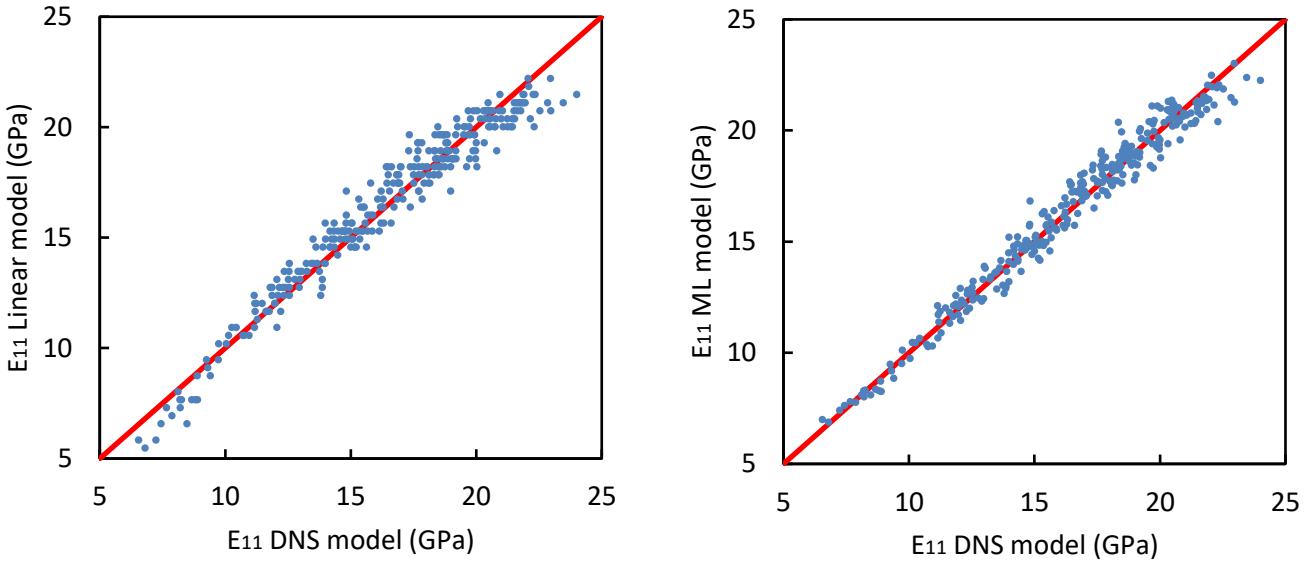

(a) Linear model (b) ML model

Figure 6. Correlation between FEA computed E_{11} and surrogate model predictions for UD RVEs samples in the test set.

The mean absolute relative error (MARE), as defined in Equation 3, was computed for each model to quantitatively evaluate their performances:

$$MARE = \frac{1}{n}\sum_{i=1}^{n}\frac{\left|E_{surrogate\ model_i} - E_{FEA_i}\right|}{E_{FEA_i}} \tag{3}$$

where n is the amount of RVEs in the test set, $E_{surrogate\ model}$ is the surrogate model predicted E_{11}, and E_{FEA} is the FEA computed E_{11}. The MARE for the linear model and the ML model are computed to be 0.043 and 0.031, respectively. The MARE is reduced 28% by including the fibre packing states into the fibre distribution characterization. The reduction in the error can also be observed from the plots in Figure 6. The results from the linear model scatter noticeably around the perfect prediction line due to the negligence of fibre packing states. By contrast, the results from the ML model are more concentrated towards the perfect prediction line.

5.2 Non-unidirectional Fibres of Varying Length

In the second case study, the database with mixed RVEs was used to investigate the performance of the proposed framework in a more general scenario. The correlation between the fibre volume fraction and the FEA computed E_{11} for all RVEs in the mixed database is plotted in Figure 7. From the plot, the FEA computed E_{11} varies significantly within the RVEs with the same fibre volume fraction due to the additional fibre distribution variables (i.e., fibre orientations and fibre lengths).

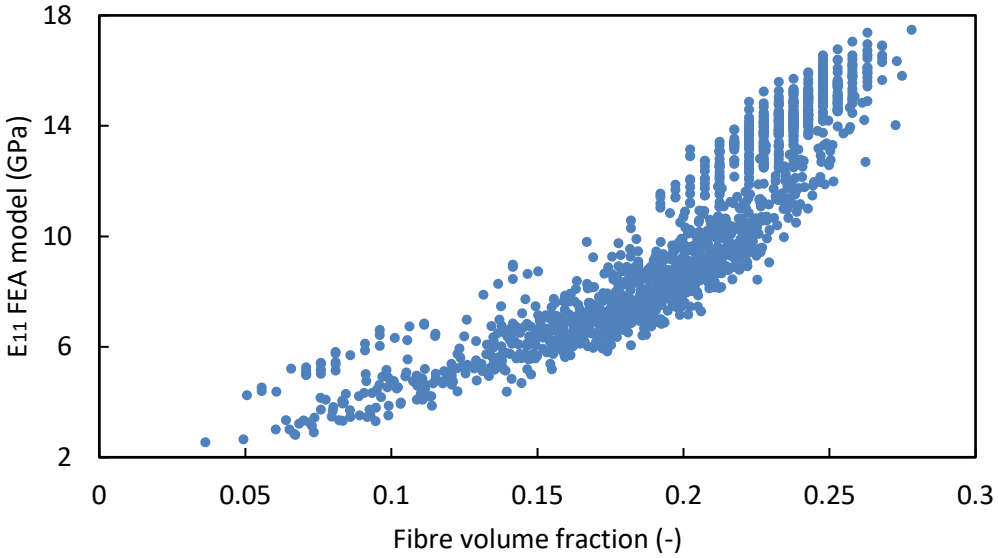

Figure 7. Correlation between fibre volume fraction and FEA computed E_{11} for mixed RVE samples.

Based on the mixed database, the ML model was trained to predict the FEA computed E_{11} in the test set. The FEA computed E_{11} versus ML model predicted E_{11} plot is shown in Figure 8, the MARE is calculated to be 0.049. The MARE is increased noticeably compared with the MARE of 0.031 from the UD case. However, the mixed database does have significantly higher variations in the E_{11} due to the introduction of the new fibre distribution variables. Compared with the variations in the mixed database shown in Figure 7, the variations in the ML model predictions shown in Figure 8 is still considerably lower. In addition, it is also needed to be considered that the amount of training data used for the mixed case (900) is significantly smaller than the number of training data used for the UD

case (2800) despite the additional fibre distribution variables introduced in the mixed case. A better performance from the ML model can be expected for the mixed database with additional data added.

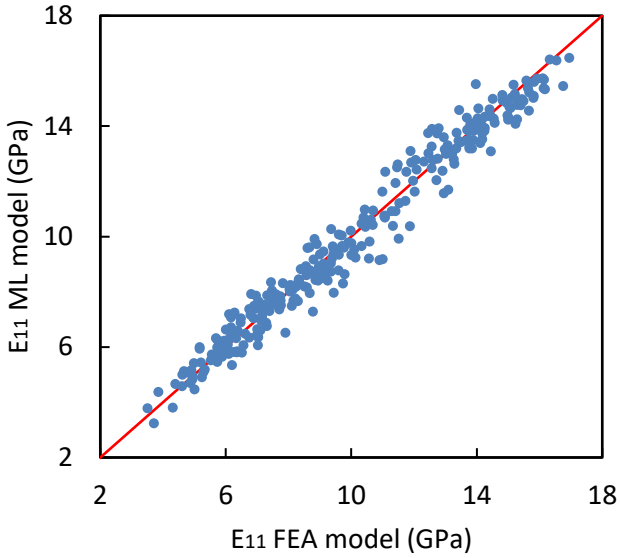

Figure 8. Correlation between FEA computed E_{11} and ML model predicted E_{11} for mixed RVEs samples in the test set.

6 CONCLUSIONS

In this study, a new fibre distribution characterization method based on the concept of fibre cell is proposed. The proposed method can characterize the fibre packing states within the DFR PMCs in addition to the fibre distribution aspects that are usually considered such as the fibre orientations and fibre lengths, and it characterizes all the fibre distribution aspects jointly rather than separately by each aspect. Then, the proposed method is integrated to an ANN to acquire the correlation between the fibre distribution and the homogenized elastic modulus. The ML framework that contains the proposed characterization method and the ANN is utilized as a surrogate model to provide fast homogenized elastic modulus predictions based on given fibre distributions.

Two case studies were performed to evaluation the proposed characterization method. In the first case study, 3400 RVEs that contain fibres with the same length and orientation was used. The results show that the homogenized elastic modulus can also be influenced by the fibre packing states, and the MARE in the homogenized elastic modulus predictions can be effectively reduced by taking the fibre packing states into consideration during fibre distribution characterization. In the second case study, 500 RVEs that contain fibres with the same length and orientation was mixed with 1000 RVEs that contain fibres with varying lengths and orientations. The results from the second case study show that the proposed characterization method can be used in a more realistic scenario where fibres with different lengths and orientations are randomly spread in the matrix, and the ML model can achieve an acceptable accuracy with a limited amount of training data. Furthermore, the proposed characterization method is also very versatile. As all fibre cell parameters are dimensionless, it can be used for characterizations in different scales and inclusions of different shapes.

7 ACKNOWLEDGEMENT

Funding from the Natural Sciences and Engineering Research Council (NSERC), the Ford Motor Company, the Research Center for High Performance Polymer and Composite Systems (CREPEC), and the McGill Engineering Doctoral Awards (MEDA) are gratefully acknowledged. This research was enabled in part by support provided by Calcul Québec (www.calculquebec.ca) and Compute Canada (www.computecanada.ca).

8 REFERENCES

[1] B. Mouhmid, A. Imad, N. Benseddiq, S. Benmedakhène, A. Maazouz. "A study of the mechanical behaviour of a glass fibre reinforced polyamide 6,6: Experimental investigation". *Polymer Testing*, 25, pp 544-552, 2006.

[2] D. Hwang, D. Cho. "Fiber aspect ratio effect on mechanical and thermal properties of carbon fiber/ABS composites via extrusion and long fiber thermoplastic processes". *Journal of Industrial and Engineering Chemistry*, 80, pp 335-344, 2019.

[3] J. Köbler, M. Schneider, F. Ospald, H. Andrä, & R. Müller. "Fiber orientation interpolation for the multiscale analysis of short fiber reinforced composite parts". *Computational Mechanics*, 61, pp 729-750, 2018

[4] K. Breuer, M. Stommel. "Prediction of Short Fiber Composite Properties by an Artificial Neural Network Trained on an RVE Database". *Fibers*, pp 8, 2021

[5] S. L. Omairey, P. D. Dunning, S. Sriramula. "Development of an ABAQUS plugin tool for periodic RVE homogenisation". *Engineering with Computers*, 35, pp 567–577, 2019.

[6] V. D. Nguyen, E. Béchet, C. Geuzaine, L. Noels. "Imposing periodic boundary condition on arbitrary meshes by polynomial interpolation". *Computational Materials Science*, 55, pp 390–406, 2012.

[7] F. Aurenhammer, R. Klein. "Chapter 5 - voronoi diagrams", in: J.-R. Sack, J. Urrutia (Eds.), *Handbook of Computational Geometry*, North-Holland, Amsterdam, pp 201–290, 2000.

[8] V. Balntas, E. Riba, D. Ponsa and K. Mikolajczyk. "*Learning local feature descriptors with triplets and shallow convolutional neural networks*". In Richard C. Wilson, Edwin R. Hancock and William A. P. Smith, editors, *Proceedings of the British Machine Vision Conference (BMVC)*, pp 119.1-119.11, 2016.

[9] J. A. Hartigan, M. A. Wong. "Algorithm as 136: A k-means clustering algorithm". *Applied Statistics*, 28, pp 100, 1979.

[10] R. Hecht-Nielsen, "Theory of the backpropagation neural network*". proceedings of the international joint conference on neural* networks, 1, pp 593–611, 1989.

[11] R. Storn, K. Price. "Differential evolution - a simple and efficient heuristic for global optimization over continuous spaces". *Journal of Global Optimization*, 11, pp 341–359, 1997.